

Characterization of poly(*N*-methylaniline) as a cathode active material in aqueous rechargeable batteries[☆]

R. Sivakumar, R. Saraswathi*

Department of Materials Science, Madurai Kamaraj University, Madurai 625021, Tamilnadu, India

Received 19 June 2001; accepted 7 September 2001

Abstract

Electrochemically deposited poly(*N*-methylaniline) (PNMA) is evaluated as a cathode active material together with a Zn anode in the fabrication of rechargeable cells in 1 M ZnSO₄ electrolyte at pH ~5. The cell shows an open-circuit voltage (OCV) of 1.35 V and a specific capacity of 25.8 Ah kg⁻¹. In a second set of experiments, the anion-exchanging PNMA is converted to a cation-exchanging electrode by sulfonation and evaluated in cells. Such an approach enhances the specific capacity of the cell by a factor of 4. The coulombic efficiency of the cell is also increased considerably. A few related experiments are performed on the parent polymer, polyaniline, to facilitate direct comparison of the results. © 2002 Elsevier Science B.V. All rights reserved.

Keywords: Poly(*N*-methylaniline); Rechargeable batteries; Self-doped polymer; Sulfonated polyaniline

1. Introduction

Conducting organic polymers are prospective cathode active materials for rechargeable batteries due to certain specific advantages such as light weight, rapid synthesis by electrodeposition and absence of electrode dissolution. Several reviews of these polymers have been published [1–4]. Polyaniline (PANI) is the most studied electroactive polymer for battery applications and has specific capacity values which range from 44 to 270 Ah kg⁻¹ [4]. A major difficulty with polyaniline is its over-oxidation during charging above 130 Ah kg⁻¹ [5]. To the authors' knowledge there has been only one report on this charge-storage application in substituted polyanilines [6]. Poly(*N*-methylaniline) (PNMA) is different from PANI because of the blocking of its proton-exchange sites by methyl substituents. In other words, PNMA can be prevented from going to the pernigraniline state, which thereby reduces the risk of over-oxidation during charging in a cell. The electrochemical preparation and redox properties of PNMA have been reported [7–17]. In this study, an account is given for the first of time the characterization of PNMA as a cathode material in aqueous cells. An attempt has also been made to convert PNMA to a self-doped polymer by covalently linking a sulfonate group

to the polymer backbone. By doing so, the usual charge-discharge mechanism of anion insertion-elimination is expected to change to a cation elimination-insertion process [18–20]. For comparative purposes, a few related experiments on polyaniline and sulfonated polyaniline have also been conducted.

2. Experimental

AR grade aniline and *N*-methylaniline were used after vacuum distillation in the presence of zinc dust. Sulfuric acid and 20% fuming sulfuric acid (AR) were used as received. All solutions were prepared with double-distilled water.

A conventional, single-compartment, three-electrode cell assembly was used to perform electrochemical experiments. For cyclic voltammetry measurements, the PANI and PNMA were directly electrodeposited (14 mC cm⁻²) on a Pt plate, while the chemically prepared sulfonated PANI (SPANI) and sulfonated PNMA (SPNMA) were dip-coated on to a Pt (1 cm²) plate by dissolving 0.6 mg of each of the polymers separately in 0.2 ml of 0.1 M ammonium hydroxide. The reference electrode was a saturated calomel electrode (SCE), and the counter electrode was a Pt foil (2 cm²). For the testing of assembled cells, PANI and PNMA were electrodeposited on a carbon substrate (using a charge of 12.8 and 25 C cm⁻², respectively). The SPANI (1.6 mg) and SPNMA (1.5 mg) were dissolved in 0.4 ml of 0.1 M

[☆]This paper is dedicated to Dr. R. Narayan, Retired Professor from the Indian Institute of Technology (IIT), Chennai.

* Corresponding author.

E-mail address: saraswathir@yahoo.com (R. Saraswathi).

ammonium hydroxide and coated on the carbon substrates (both 3 cm^2). The anode was an amalgamated Zn plate.

The electrochemical experiments were performed with an EG & G, PAR potentiostat/galvanostat (model 263A). Impedance studies were carried out with an EG & G, PAR (model 6310) electrochemical impedance analyzer. IR spectra of the four polymer samples were recorded with a Jasco (model 410) FT-IR spectrophotometer. Scanning electron micrographs (Hitachi model 450) were obtained for thin films of PANI and PNMA deposited on indium–tin oxide substrates whereas powder samples were used for SPANI and SPNMA.

3. Results and discussion

3.1. Preparation of polymers

Thick films of PANI could be electrodeposited on a carbon substrate from an aqueous electrolyte of 0.5 M aniline and 0.5 M sulfuric acid by potentiostatic control at 0.65 V versus SCE. On the other hand, a constant-current (2 mA cm^{-2}) method had to be employed to obtain uniform adherent films of PNMA using a monomer and acid concentrations of 1 M each. The polymers were obtained in the doped state. The PANI sample gave a conductivity of 12 S cm^{-1} , while PNMA showed a value of 0.1 S cm^{-1} .

The self-doped sulfonated polymers were prepared as follows. PANI was obtained by chemical polymerization of aniline (0.1 M) in the presence of 0.5 M sulfuric acid using ammonium persulfate at 0°C [21]. The product, emeraldine salt, was washed well in double-distilled water and dried in vacuum. It was then stirred with 1 M sodium hydroxide for 2 h to give the emeraldine base (EB) form. The EB was then sulfonated using the procedure reported elsewhere [22]. In this procedure, $\sim 0.5 \text{ g}$ of EB was treated with 2.5 ml of phenylhydrazine for 1 h, washed with ether, and dried. This was then treated with 10 ml of 20% fuming sulfuric acid (pre-cooled to $\sim 5^\circ \text{C}$) for 1 h. The resultant solution was poured into an ice–water mixture, filtered, and dried. A similar procedure was adopted to prepare SPNMA from the chemically processed PNMA sample. The measured conductivity values were 4.7×10^{-3} and $1.2 \times 10^{-4} \text{ S cm}^{-1}$ for SPANI and SPNMA, respectively.

3.2. Characterization of polymers

The FT-IR spectra of the four polymer samples used in this study are shown in Fig. 1. The spectral features all have the general characteristics of PANI [23]. The common are for aromatic stretching (1492 and at 1566 cm^{-1} for C=C in quinoid and benzenoid rings, respectively) and C–H bending at 822 cm^{-1} for para-coupling of the aniline rings. The presence of a strong band at 1117 cm^{-1} in the spectra of PANI and PNMA corresponds to the sulfate dopant. In the case of the sulfonated polymer samples, the bands at 618 , 1025 and 1065 cm^{-1} are due to sulfonate stretching [24–26].

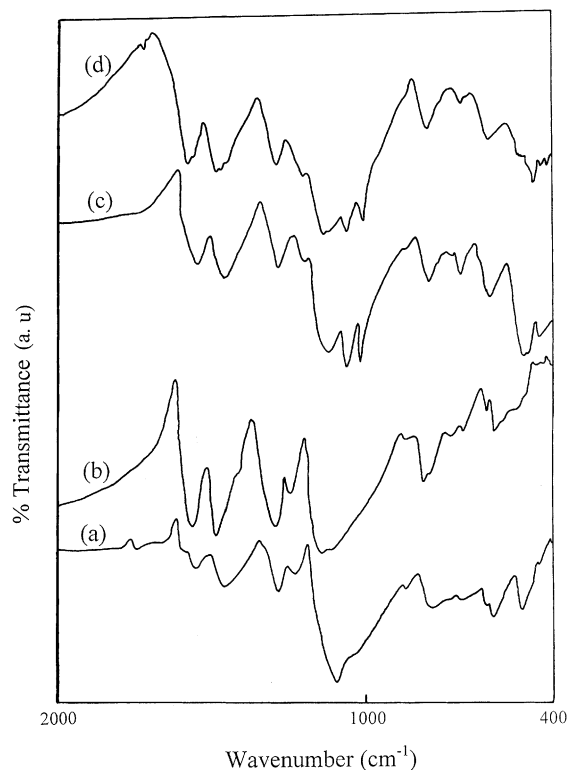


Fig. 1. FT-IR spectra of (a) PANI, (b) PNMA, (c) SPANI, (d) SPNMA.

Scanning electron micrographs of the four polymer samples are presented in Fig. 2. A granular morphology has been observed for PANI films [27]. By contrast, the PNMA film exhibits a more compact and smooth morphology. Both the sulfonated polymeric powder samples display a dense morphology. Wei et al. [22] have reported a globular structure of $20 \mu\text{m}$ in size for a SPANI film deposited on a silicon substrate. It is inferred from these morphological studies that PNMA, SPANI and SPNMA will be more suitable for use in batteries than granular PANI.

Cyclic voltammograms of thin films of the four polymers were recorded using an electrolyte solution of 1 M Na_2SO_4 adjusted to various pH values by the addition of sulfuric acid. The data obtained at pH ~ 5 are given in Figs. 3 and 4. The results show that unlike PANI, which has been reported to lose its electroactivity above pH 4 [28], PNMA retains its electroactivity even up to a pH of 7. Although, the cathodic and anodic peak current values of PNMA decrease at still higher pH values, the peak shapes remain the same. The cyclic voltammograms of both the sulfonated polymer films show well-defined redox peaks at all pH values. The complete details of the effects of pH on all the four polymers will be reported elsewhere.

The polymer films were switched back and forth between the reduced and oxidized states in order to establish the rechargeability of the cells. It is interesting to note that the SPNMA is able to withstand a greater number of such cycles at pH ~ 5 without much loss of redox charge as can be seen

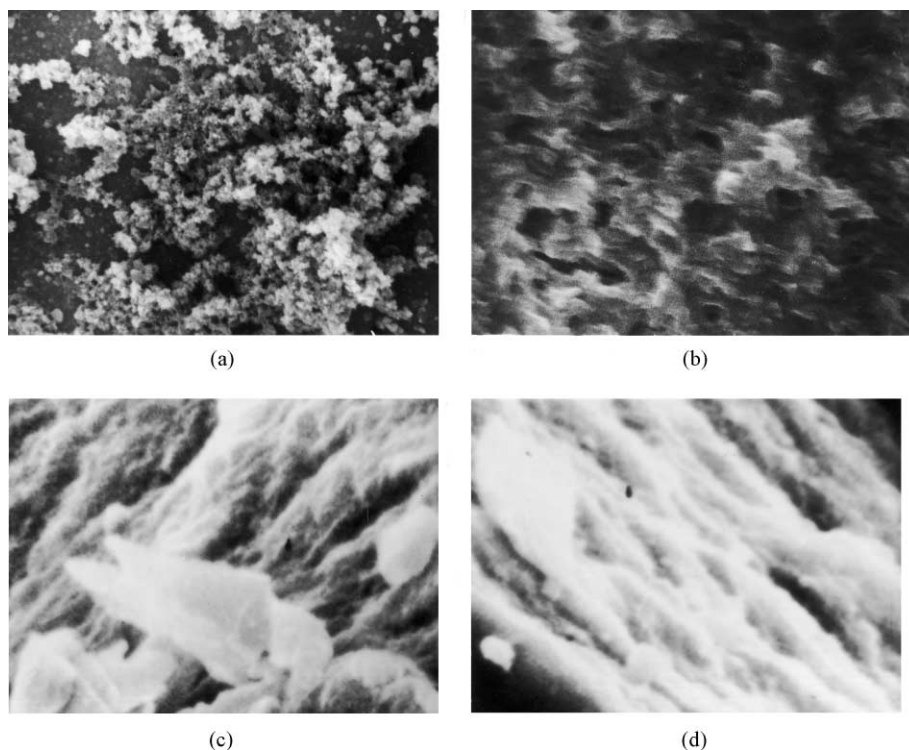


Fig. 2. Scanning electron micrographs of (a) PANI, (b) PNMA, (c) SPANI, (d) SPNMA. Magnification is 3000 \times .

from the comparative chart shown in Fig. 5. The redox charge of SPNMA decreased by about 8% over 200 cycles.

3.3. Charge–discharge behavior

3.3.1. PANI and PNMA

Cells were assembled with PANI and PNMA as cathodes and with Zn as an anode in an aqueous electrolyte solution of 1 M ZnSO₄ at pH 5. These two polymers are of p-type viz., anion-doped. The charging and discharging processes at the polymer cathode involves a simple insertion and elimination

of the sulfate dopant. At the anode, Zn deposits during charging and dissolves during discharging (Scheme 1).

The variation in the open-circuit voltage (OCV) of the four cells is shown in Fig. 6 as a function of time. The cell OCV decreased rapidly for up to about 1 h, and then remained stable for over a tested period of 3 days of standing. Typical charge–discharge curves for PANI and PNMA cells are shown in Figs. 7 and 8, respectively. The curves are almost symmetrical with respect to the switching potentials. Care has been exercised not to over-oxidize the polymers. The charging potential was limited to 1.5 V while

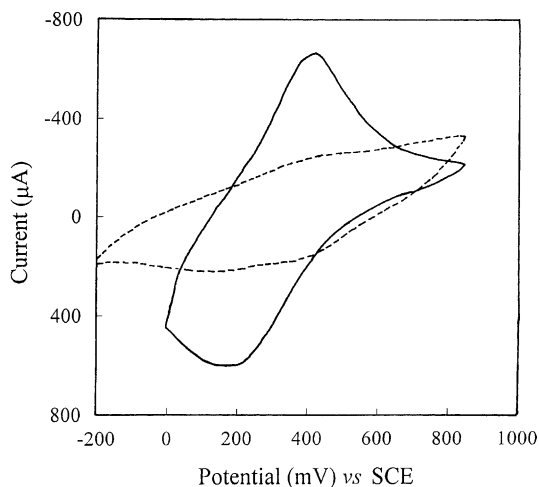


Fig. 3. Cyclic voltammograms of PANI (dotted line) and PNMA (solid line) in 1 M Na₂SO₄ electrolyte solution at pH \sim 5; scan rate 20 mV s⁻¹.

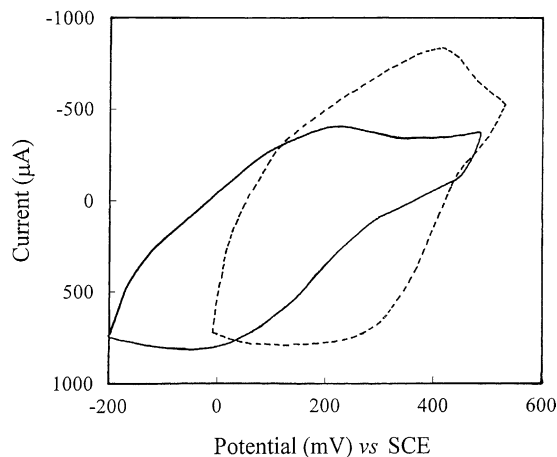


Fig. 4. Cyclic voltammograms of SPANI (dotted line) and SPNMA (solid line) in 1 M Na₂SO₄ electrolyte solution at pH \sim 5; scan rate 20 mV s⁻¹.

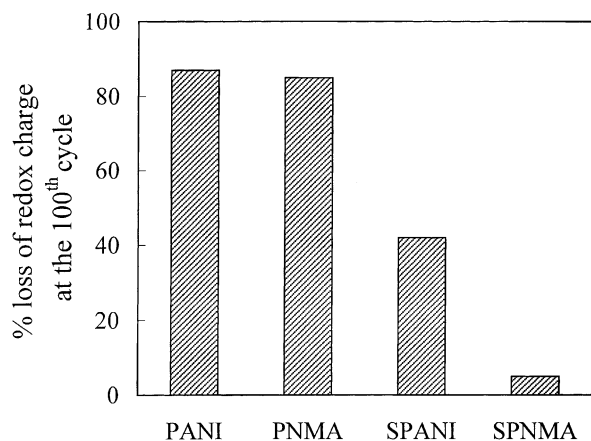
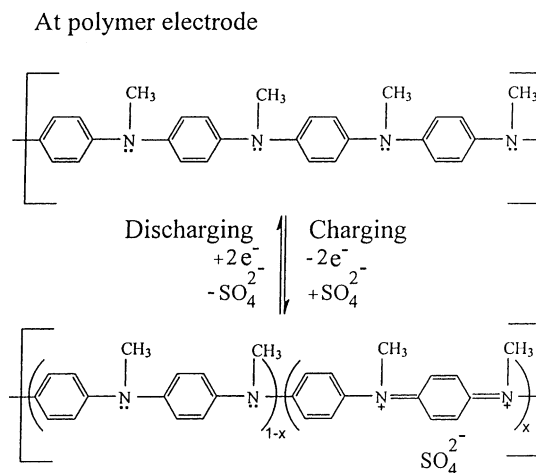
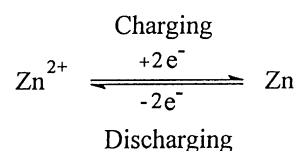


Fig. 5. Comparative chart showing percent loss of redox charge at 100th cycle for PANI, PNMA, SPANI and SPNMA by repeated cycling between -0.2 and 0.525 V (SCE) at a scan rate of 20 mV s^{-1} in $1 \text{ M Na}_2\text{SO}_4$ electrolyte solution at $\text{pH} \sim 5$.

the discharging potential did not exceed 0.9 V. The calculated cell parameters are given in Table 1 along with the reported literature values for PANI [29–32] and poly(2-methylaniline) [6] cells. The present study yielded a specific capacity of 59 Ah kg^{-1} for the PANI cell instead of the widely reported 100 Ah kg^{-1} . The specific capacity values decrease markedly if the weight of the doped polymer in the charged state is taken into account in the calculations instead of the polymer weight in the discharged state. For example, assuming a 25% sulfate dopant level in the polymer, a 20% decrease in specific capacity is expected. A specific capacity of 25.8 Ah kg^{-1} is found for the PNMA cells, which is nearly half of the value obtained for the PANI cells. It is



At Zn electrode



Scheme 1. Schematic representation of the charge–discharge process in a Zn/1 M ZnSO_4 ($\text{pH} \sim 5$)/PNMA rechargeable cell.

noted that the discharge curves of PNMA are somewhat different from those of PANI, in that a distinct kink at about 1 V is present.

Measurements were made of the ac impedance of the PNMA cell at various applied dc potentials in the frequency range from 100 kHz to 0.1 Hz , the results are presented

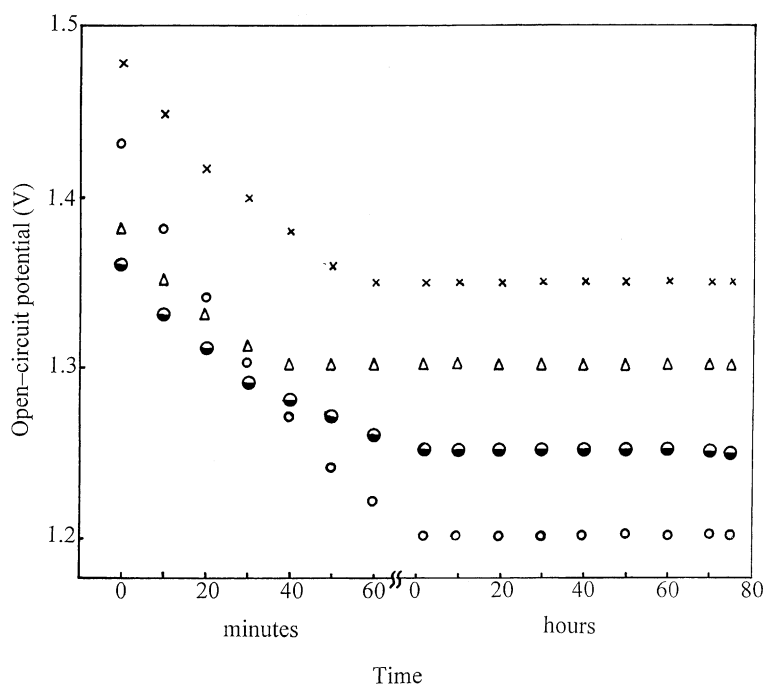


Fig. 6. Variation of OCV of assembled cells against time: PANI (○), PNMA (×), SPANI (△) and SPNMA (●).

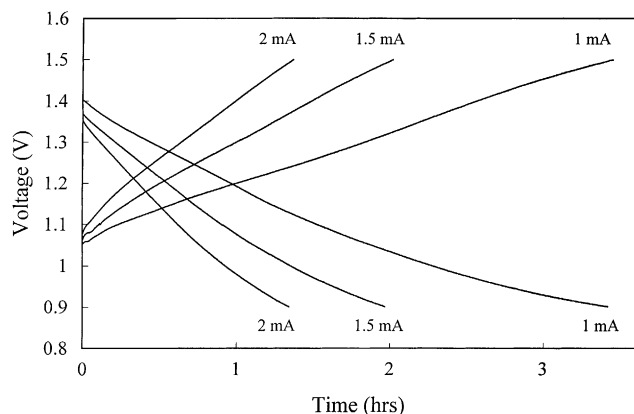


Fig. 7. Charge–discharge behavior of Zn/1 M ZnSO₄ (pH ~ 5)/PANI cell at various current ratings.

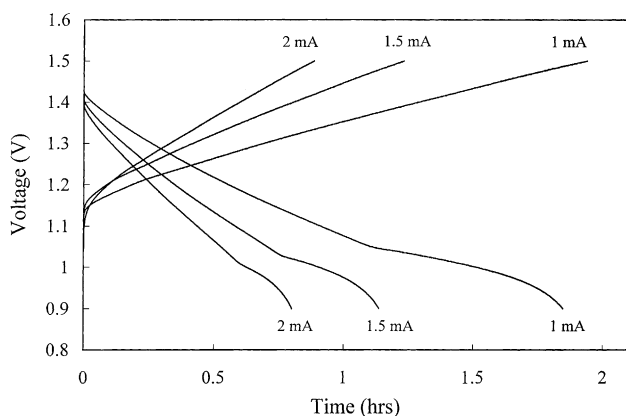


Fig. 8. Charge–discharge behavior of Zn/1 M ZnSO₄ (pH ~ 5)/PNMA cell at various current ratings.

in Fig. 9. At all potentials, the complex impedance plots show a semicircle in the high-frequency region followed by a prominent line in the low-frequency region. The semicircle indicates charge transfer domination and is characteristic of

a parallel network formed by a resistor and a capacitor, as represented in Fig. 10(a). The double-layer capacitance (C_{dl}) calculated from the data at 1.4 V (peak potential) is $1.46 \times 10^{-5} \text{ F cm}^{-2}$. The charge-transfer resistance (R_{ct}) corresponds to the diameter of the semicircle which decreases from 3.37Ω at 0.9 V to 1.4Ω at 1.7 V. The solution resistance (R_s) which corresponds to the intercept at the highest measurement frequency on the real part of the impedance axis (X -axis) does not vary with the applied dc potential in the initial narrow potential region between 0.9 and 1.1 V. The R_s jumps from 9.6 to 21.5Ω at 1.4 V, however, and then remains virtually constant with further increase in applied potential. The line following the semicircle corresponds to a Warburg impedance, caused by the diffusion of sulfate dopant ions into the polymer film. The Randles equivalent circuit shown in Fig. 10(a) can be modified to include the Warburg impedance (Z_w) as a cell component (Fig. 10(b)). In the present set of experiments, the complex impedance plots show a small closed loop in the frequency range between 1 kHz and 1 Hz, particularly in the peak potential region (1.4–1.7 V versus Zn). To our knowledge, this type of impedance behavior has not been reported for electroactive polymer films. A search of the literature for such an observation yielded three papers which had reported the possibilities of the occurrence of such secondary loops in the impedance plots of Li-ion cells [33–35]. The origin of such impedance loops was discussed in terms of the contribution of both the cathode and the anode in the discharge process. There have been a number of reports on the impedance analysis of electroactive polymer films [3,36–43]. Some studies show that the ideal thickness of the polymer film for observing all three regions, viz., kinetic control, diffusion control and charge saturation, in the impedance plot is about $0.5 \mu\text{m}$ or less. From impedance data, Kanamura et al. [40] have calculated a diffusion coefficient of $0.64 \times 10^{-12} \text{ cm}^2 \text{ s}^{-1}$ for BF_4^- anions in a PANI solid matrix [43]. Assuming a similar value for the sulfate anion in the PNMA film, the film thickness is

Table 1

Comparison of cell parameters of aqueous PANI cells reported in literature with the values obtained in present study

Cathode	Anode	Electrolyte	OCV (V)	Specific capacity (Ah kg ⁻¹)	Coulombic efficiency (%)	Reference
PNMA	Zn	1 M ZnSO ₄ (pH = 5)	1.35	25.8	98	Present study
PANI	Zn	1 M ZnSO ₄ (pH = 5)	1.2	59	99	Present study
SPNMA	Zn	1 M ZnSO ₄ (pH = 5)	1.25	105	150	Present study
SPANI	Zn	1 M ZnSO ₄ (pH = 5)	1.3	105	110	Present study
PANI	Zn	1 M ZnSO ₄	<1.35	108	~100	[29]
PANI	Zn	ZnSO ₄	–	100	~100	[30]
PANI	Zn	Saturated ZnCl ₂ + 1 M NH ₄ Cl	>1.1	60–86	87–94	[31]
PANI	Zn	2 M ZnBr ₂ + 1 M NH ₄ Cl	1.5	90–95	73–99	[32]
Poly(2-methylaniline)	Zn	1.5 M ZnCl ₂ (pH = 2.68)	1.3	106.6	100	[6]

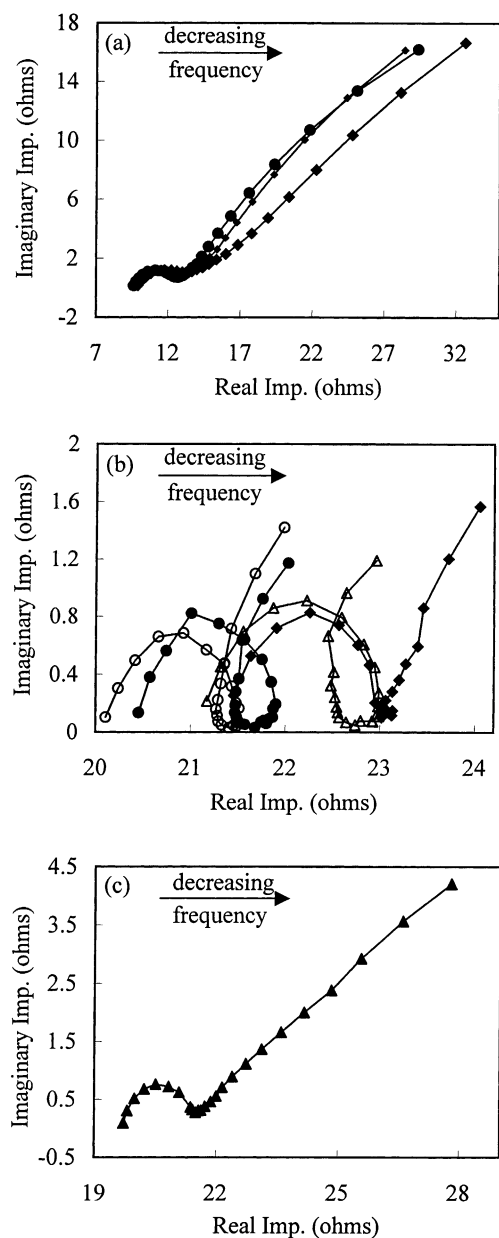


Fig. 9. Impedance spectra of Zn/1 M ZnSO₄ (pH ~ 5)/PNMA cell at various applied dc potentials: (a) 0.9 V (◆), 1 V (●), 1.1 V (◊); (b) 1.4 V (◆), 1.5 V (△), 1.6 V (●), 1.7 V (○); (c) 1.8 V (▲) vs. Zn.

expected to play a prominent role in controlling the diffusion process. We have carried out impedance experiments for somewhat thicker PNMA films (~50 μm) deposited on a carbon substrate, as used in the above measurements of cell discharge. The impedance loop in the peak potential region is possibly associated with a delay in the dopant diffusion into the solid polymer matrix.

3.3.2. SPANI and SPNMA

The concept of self-doping in conducting polymers was first introduced by Yue and Epstein [44]. They described the synthesis of a self-doped conducting PANI, in which a

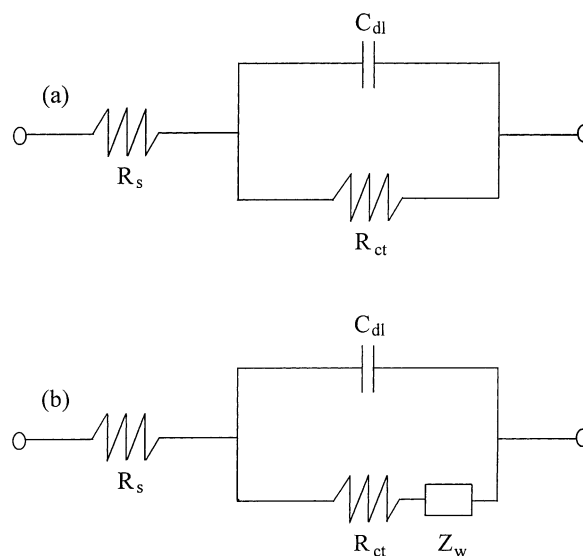
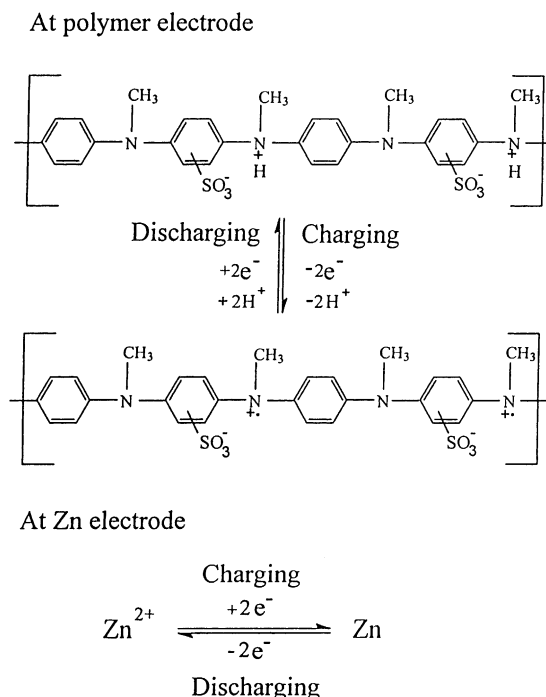


Fig. 10. Randles equivalent electrical circuit depicting (a) kinetic control and (b) kinetic control and diffusion processes of Zn/ZnSO₄/PNMA cell (R_s = solution resistance; C_{dl} = double-layer capacitance; R_{ct} = charge-transfer resistance and Z_w = Warburg impedance).

sulfonic acid group was introduced on alternative aniline rings. Since then, several other studies have been published [18,22,24,45] on self-doped polyanilines and have reported different synthetic routes for the sulfonation of PANI and the characterization of the resultant polymers. Recently, Shimizu et al. [46] have devised a method to prepare SPANI from a sulfonic acid substituted aniline by means of a chemical method. They identified the usefulness of self-doped SPANI in lithography. Barbero et al. [19,20,25] have suggested that these polymers can be used as cation-insertion electrodes for battery applications. They established the ion-exchange mechanism of SPANI by means of the modern techniques of electrochemical quartz crystal microbalance and probe beam deflection, and also brought out the salient differences between the SPANI and PANI with respect to the redox properties at different pH values. It is now understood that by fixing a negative group such as $-\text{SO}_3^-$ to the polymer backbone, the anion-exchange redox mechanism can be changed to a proton-exchange process in aqueous electrolytes, and to a cation-exchange (Li^+) mechanism in non-aqueous electrolytes.

For the first time, an attempt is made here to prepare SPNMA and study its usefulness as a battery material. The following is a summary of the results obtained.

As described above, the cells were assembled with SPANI or SPNMA as cathodes and with Zn as anode using an aqueous electrolyte solution of 1 M ZnSO₄. The charge-discharge mechanism is different, and is shown in Scheme 2. There is no anion-insertion process during charging. Instead, the sulfonated polymers eliminate the protons and the negatively charged sulfonate group counteracts the positive charge created on the polymer during oxidation. The reverse is true for the discharge process.



Scheme 2. Schematic representation of the charge–discharge process in a Zn/1 M ZnSO₄ (pH ~ 5)/SPNMA rechargeable cell.

Charge–discharge curves for SPANI and SPNMA are shown in Figs. 11 and 12, respectively. An interesting observation here is the longer discharge time compared with the charging time. This will enhance the coulombic efficiency of the cell. Both cells were charged to 1.4 V and discharged to 0.65 V at different current ratings. The OCV of the SPNMA cell is 1.25 V. The specific capacity is 105 Ah kg⁻¹, which is nearly four times higher than the value obtained with for the PNMA cell. The OCV of the SPANI cell is 1.3 V and the specific capacity is 105 Ah kg⁻¹, which is nearly twice that of the PANI cell. It may be noted that Barbero et al. [20] reported a specific charge of 37 Ah kg⁻¹ for SPANI in aqueous solution and 68 Ah kg⁻¹ in non-aqueous media. These values were obtained, how-

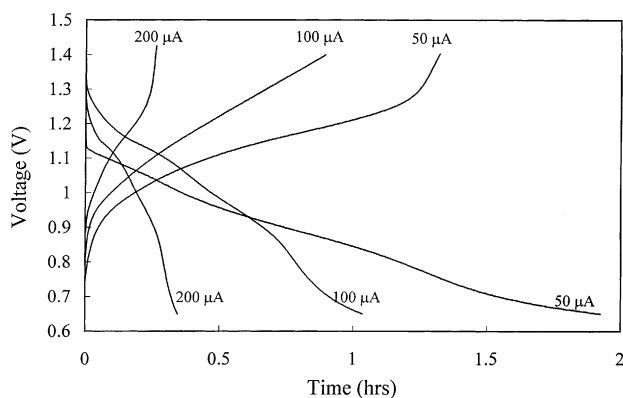


Fig. 11. Charge–discharge behavior of Zn/1 M ZnSO₄ (pH ~ 5)/SPANI cell at various current ratings.

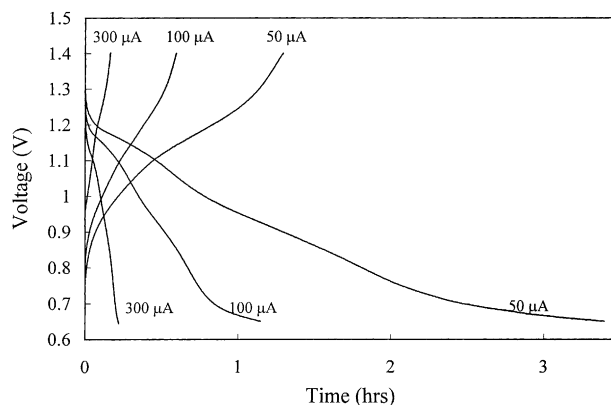


Fig. 12. Charge–discharge behavior of Zn/1 M ZnSO₄ (pH ~ 5)/SPNMA cell at various current ratings.

ever, from a calculation involving cyclic voltammetric redox charge and polymer mass and not from actual cell-discharge experiments.

4. Conclusions

PNMA is characterized as a cathode active material in aqueous rechargeable cells. Sulfonation of the polymer causes nearly four-fold enhancement of the specific capacity of the cell. Also, SPNMA has a better rechargeability compared with PNMA.

Acknowledgements

The authors gratefully acknowledge the Department of Science and Technology for a financial grant (sp/s1/H-32/95) for this work.

References

- [1] M. Morishita, S. Abe, *Electrical Eng. Jpn.* 5 (1987) 107.
- [2] K.S.V. Santhanam, N. Gupta, *Trends. Poly. Sci.* 1 (1993) 284.
- [3] B. Scrosati, *Application of Electroactive Polymers*, 1st Edition, Chapman & Hall, London, 1993.
- [4] P. Novak, K. Muller, K.S.V. Santhanam, O. Haas, *Chem. Rev.* 97 (1997) 207.
- [5] S. Taguchi, T. Tanaka, *J. Power Sources* 20 (1987) 249.
- [6] M. Shaolin, Q. Bidong, *Synth. Met.* 32 (1989) 129.
- [7] N. Oyama, T. Ohsaka, *Synth. Met.* 18 (1987) 375.
- [8] N. Comisso, S. Daolio, G. Mengoli, R. Salmaso, S. Zecchin, G. Zotti, *J. Electroanal. Chem.* 255 (1988) 97.
- [9] J.J. Langer, *Mater. Sci.* 14 (1988) 41.
- [10] S.K. Manohar, A.G. Macdiarmid, *Synth. Met.* 29 (1989) E349.
- [11] A. Watanabe, K. Mori, A. Iwabuchi, Y. Iwasaki, Y. Nakamura, O. Ito, *Macromolecules* 22 (1989) 3521.
- [12] J.J. Langer, *Synth. Met.* 35 (1990) 295.
- [13] J.J. Langer, *Synth. Met.* 35 (1990) 301.
- [14] C. Barbero, M.C. Miras, O. Haas, R. Kotz, *J. Electroanal. Chem.* 310 (1991) 437.
- [15] G.D. Aprano, M. Lecrec, G. Zotti, *Macromolecules* 25 (1992) 2145.

- [16] J.W. Chevalier, J.Y. Bergeron, L.H. Dao, *Macromolecules* 25 (1992) 3325.
- [17] J. Yano, M. Kokura, K. Ogura, *J. Appl. Electrochem.* 24 (1994) 1164.
- [18] J. Yue, Z.H. Wang, K.R. Cromack, A.J. Epstein, A.G. MacDiarmid, *J. Am. Chem. Soc.* 113 (1991) 2665.
- [19] C. Barbero, M.C. Miras, R. Kotz, O. Hass, *Synth. Met.* 55–57 (1993) 1539.
- [20] C. Barbero, M.C. Miras, R. Kotz, O. Hass, *J. Electroanal. Chem.* 437 (1997) 191.
- [21] D. Muller, M. Jozefowicz, *Bull. Soc. Chim. Fr.* 11 (1972) 4083.
- [22] X.L. Wei, Y.Z. Wang, S.M. Long, C. Bobeczko, A.J. Epstein, *J. Am. Chem. Soc.* 118 (1996) 2545.
- [23] Y. Cao, S. Li, Z. Xue, D. Guo, *Synth. Met.* 16 (1986) 305.
- [24] J. Yue, A.J. Epstein, A.G. Macdiarmid, *Mol. Cryst. Liq. Cryst.* 189 (1990) 255.
- [25] C. Barbero, M.C. Miras, B. Schnyder, O. Haas, R. Kotz, *J. Mater. Chem.* 4 (1994) 1775.
- [26] D. Lin-Vien, N.B. Colthup, W.G. Fateley, J.G. Grasselli, *The Handbook of Infrared and Raman Characteristic Frequencies of Organic Molecules*, Academic Press, London, 1991.
- [27] B. Wang, J. Tang, F. Wang, *Synth. Met.* 13 (1986) 329.
- [28] T. Hirai, S. Kuwabata, H. Yoneyama, *J. Chem. Soc., Faraday Trans. 1* (85) (1989) 969.
- [29] A. Kitani, M. Kaya, K. Sasaki, *J. Electrochem. Soc.* 133 (1986) 1069.
- [30] N. Koura, T. Kijima, *Denki Kagaku* 55 (1987) 386.
- [31] B. Wang, G. Li, F. Wang, *J. Power Sources* 24 (1988) 115.
- [32] G. Mengoli, M.M. Musiani, D. Pletcher, S. Valcher, *J. Appl. Electrochem.* 17 (1987) 515.
- [33] P.O. Braatz, K.C. Lim, A.M. Luckner, W.H. Smith Jr., J.D. Margenum, H.S. Lim, *ECS Extended Abstracts* 97 (1997) 121.
- [34] K. Ozawa, *Solid State Ionics* 69 (1994) 212.
- [35] G. Nagasubramanian, *J. Power Sources* 87 (2000) 226.
- [36] S.H. Glarum, J.H. Marshall, *J. Electrochem. Soc.* 134 (1987) 142.
- [37] G. Mengoli, M.M. Musiani, D. Pletcher, S. Valcher, *J. Appl. Electrochem.* 17 (1987) 525.
- [38] I. Rubinstein, E. Sabatani, J. Rishpon, *J. Electrochem. Soc.* 134 (1987) 3078.
- [39] T.B. Hunter, P.S. Tyler, W.H. Smyrl, H.S. White, *J. Electrochem. Soc.* 134 (1987) 2198.
- [40] K. Kanamura, Y. Kawai, S. Yonezawa, Z. Takehara, *J. Electrochem. Soc.* 142 (1995) 2894.
- [41] A. Lian, S. Besner, L.H. Dao, *Synth. Met.* 74 (1995) 21.
- [42] R. Saraswathi, M. Gerard, B.D. Malhotra, *J. Appl. Poly. Sci.* 74 (1999) 145.
- [43] J. Bobacka, A. Lewenstam, A. Ivaska, *J. Electroanal. Chem.* 489 (2000) 17.
- [44] J. Yue, A.J. Epstein, *J. Am. Chem. Soc.* 112 (1990) 2800.
- [45] J. Yue, G. Gordon, A.J. Epstein, *Polymer* 33 (1992) 4410.
- [46] S. Shimizu, T. Saitoh, M. Uzawa, M. Yuasa, K. Yano, T. Maruyama, K. Watanabe, *Synth. Met.* 85 (1997) 1337.